

Manuscript Number: CAMWA-D-17-01692R1

Title: A Two-Grid Decoupled Algorithm for Fracture Models

Article Type: Regular Article

Keywords: Fracture model; two-grid method; decoupling; Darcy's law;
Darcy-Forchheimer's law

Abstract: In this paper, we consider a two-grid decoupled algorithm for two categories of fracture models. In the mixed Darcy/Darcy fracture model, fluid flow in fractures as well as in the surrounding medium is governed by Darcy's law. And in the mixed Darcy-Forchheimer/Darcy fracture model, flow in fractures is governed by Darcy-Forchheimer's law while that in surrounding matrix is governed by Darcy's law. In the proposed two-grid method, we use a coarse grid approximation to the interface coupling conditions for decoupling mixed problems in fractures and surrounding matrix. Error estimates show that the two-grid decoupled algorithm retains the same order of approximation accuracy as the coupled algorithm for the pressure p on H^1 semi-norm and the velocity u on $(L^2)^2$ norm. Numerical experiments are carried out to verify the accuracy and efficiency of the decoupled algorithm, in which the computation times are reduced greatly compared to the coupled method.

April 28, 2018

Re: Paper Number: CAMWA-D-17-01692

Title: A Two-Grid Decoupled Algorithm for Fracture Models

Authors: Shuangshuang Chen, Hongxing Rui

Dear Editor:

Please find enclosed the revised version of the paper Referenced CAMWA-D-17-01692. We have revised the paper along the guidelines of anonymous reviewers. All their suggestions and concerns have been addressed in this version that we hope to be acceptable.

We would like to thank you and the anonymous reviewers for their efforts that helped us to improve the quality of this paper.

Yours sincerely,

Shuangshuang Chen, Hongxing Rui

Authors' Responses to Reviewers' Comments

Paper Number: CAMWA-D-17-01692

Title: A Two-Grid Decoupled Algorithm for Fracture Models

Authors: Shuangshuang Chen, Hongxing Rui

We would like to give thanks to the referees for their comments and suggestions. Those comments are all valuable and very helpful for revising and improving our paper, as well as the important guiding significance to our researches. We have studied comments carefully and have revised the manuscript taking the reviewers' suggestions and concerns into consideration. The details of the changes are explained below.

Reviewer No. 1:

1. Comment: This paper applied the two-grid technique to decouple the algorithms for two kinds of fracture models, i.e., a model coupled with Darcy flow and a model coupled with Darcy-Forchheimer flow. The main contribution of this paper is that the computation time of the proposed two-grid decoupling algorithm reduced greatly comparing with the traditionally coupled algorithm. Besides, they also analyzed the error estimates for the model coupled with Darcy flow. That the convergence rate of the pressure and velocity are optimal. The referee find results of this paper are interesting to be published in Computers and Mathematics with Applications. Some improvements of the English writing and paper organization are recommended in the second reversion. Some of them are listed below.

Response: Thank you for your comments and suggestions. We have revised the paper following your comments as detailed below.

2. Comment: The second and third lines of the abstract is difficult to read. The description of the two models is not clear. Please rewrite it.

Response: Thank you for your comments and suggestions. In the abstract of our paper, we rewrite the description of the two models as follows. "In this paper, we consider a two-grid decoupled algorithm for two categories of fracture models. In the mixed Darcy/Darcy fracture model, fluid flow in fractures as well as in the surrounding medium is governed by Darcy's law. And in the mixed Darcy-Forchheimer/Darcy fracture model, flow in fractures is governed by Darcy-Forchheimer's law while that in surrounding matrix is governed by Darcy's law." Please see it in the abstract of the first page.

3. Comment: In the 5th line of introduction in Page 1 (in the original version), "very smaller" might should be "a very small".

Response: Thank you for your comments and suggestions. We have revised this, and change "very smaller" to "a very small". Please see it in 8th line of introduction in the first page (in the revised version).

4. Comment: In the 9th line in Page 2 (in the original version), it would be much better to use "aforementioned" instead of "above mentioned".

Response: Thank you for your comments and suggestions. We have revised it, and we replace "above mentioned" by "aforementioned". Please see it in the 16th line in Page 2 (in the revised version).

5. Comment: In the 2nd line of section 2 in Page 3, "in the fracture" is recommended to be "on the fracture".

Response: Thank you for your comments and suggestions. We have revised it, and we change "in the fracture" to "on the fracture". Please see it in the 2nd line of section 2 in Page 3.

Reviewer No. 2:

1. Comment: In this paper, the authors propose a two-grid method for decoupling fracture models. Two flow models, namely the Darcy and Darcy-Forchheimer models, for the fluids in fracture are considered. Using this decoupling method, problems in the matrix domains and the fracture domains on the fine grid are formulated and solved separately; the original coupled problem is solved on the coarse grid only. The authors show the optimal convergence rates of the proposed method for pressure p and velocity u . Numerical experiments confirm the theoretical analysis. The discussion of the paper is clear; and the overall quality of the paper is good. We recommend this paper to be published on CAMWA with some minor revisions; detailed comments are listed as follows.

Response: Thank you for your comments and suggestions. We have revised the paper following your comments as detailed below.

2. Comment: Page 3: Abuse of notation – d denotes both the boundary of and thickness of the fracture.

Response: Thank you for your comments and suggestions. In the first paragraph of Section 2, we rewrite the computational domain as follows: $\Omega = [a_1, a_2] \times [b_1, b_2]$, and we have revised all the relevant part where it is used. In this paper, d refers to the width of fracture. Please see it in the first paragraph of Section 2.

3. Comment: Page 5, line 4 (in the original version): “ $-2(1 - \xi)$ ” should be “ $+2(1 - \xi)$ ”.

Response: Thank you for your comments and suggestions. We have revised “ $-2(1 - \xi)$ ” as “ $+2(1 - \xi)$ ”. Please see it in the 9th line in Page 5 (in the revised version).

4. Comment: Page 5 (in the original version): “ Ω ” should be “ Ω_i in definition of W_i^h ”.

Response: Thank you for your comments and suggestions. We have revised it, and we change “ Ω ” to “ Ω_i ” in definition of W_i^h . Please see it in Page 6, line 6 (in the revised version).

5. Comment: Page 5 (in the original version): “ $\partial\Omega$ ” should be “ Γ_i in definition of W_i^h ”.

Response: Thank you for your comments and suggestions. We have revised “ $\partial\Omega$ ” as “ Γ_i ” in definition of W_i^h . Please see it in Page 6, line 6 (in the revised version).

6. Comment: Page 6: “ $(1 - \xi)$ ” should be “1” in the 6th item of (3.3)? It is confusing why this coefficient comes up.

Response: Thank you for your comments and suggestions. We have revised it. We change “ $(1 - \xi)$ ” to “1” in the sixth item of (3.3). Please see it Page 6.

7. Comment: Page 8: “ $(1 - \xi)$ ” should be “1” in the 6th item of (4.7) (in the original version)? Same as above.

Response: Thank you for your comments and suggestions. We have revised “ $(1 - \xi)$ ” as “1” in the sixth item of (4.8) (in the revised version). Please see it in Page 9 (in the revised version).

8. Comment: “ p_i^h ” should be “ p_{i+1}^h ” in the 1st item of right hand of (4.7) (in the original version).

Response: Thank you for your comments and suggestions. We have revised it, and we change “ p_i^h ” to “ p_{i+1}^h ” in the 1st item of right hand of (4.8) (in the revised version). Please see it in Page 9 (in the revised version).

9. Comment: Page 10, line 8 (in the original version): missing vector transpose symbol “ T ”.

Response: Thank you for your comments and suggestions. We add the vector transpose symbol “ T ”. Please see it in the 6th line under Equation (5.2) in Page 10 (in the revised version).

Reviewer No. 3:

1. Comment: The manuscript of Chen and Rui titled “A Two-Grid Decoupled Algorithm for Fracture Models”, can potentially fit in the aims and scope of the journal. However, the paper is poorly structured and not well-written. In addition, there are numerous grammatical errors and spelling mistakes.

Response: Thank you for your comments and suggestions. We have revised them.

The paper has been restructured as follows.

Section 1: Introduction. In the first paragraph of this section, we introduce briefly the mixed Darcy/Darcy

fracture model and the mixed Darcy-Forchheimer/Darcy fracture model and numerical methods for two fracture models are added; In the second paragraph, we introduce the development of the two-grid decoupled algorithm and describe its basic idea; In the third paragraph, we describe our work of this paper, and add the advantages of the proposed method; In the last paragraph of introduction, we give the outline of this paper. Please see it in Pages 1-3.

Section 4: Error estimate. In the first paragraph, we firstly describe the main goal of this section. Then theoretical analysis of the coupled method for the mixed Darcy/Darcy fracture model is presented in Theorem 4.1. Based on Theorem 4.1, the theoretical result of the proposed two-grid decoupled algorithm is derived in Theorem 4.2.

Section 6: Numerical experiment. Numerical experiments are carried out for both mixed Darcy/Darcy fracture model and Darcy-Forchheimer/Darcy fracture model. We add the conclusion of numerical results for each fracture model. Please see them in Pages 15-16.

Section 7: Conclusion. We add the conclusion of our work in this paper, and we further emphasize the advantages of the proposed two-grid decoupled method for fracture models. Please see it in Page 17.

We also revise grammatical errors and spelling mistakes. For example,

- We change “The permeabilities of fractures are much higher or lower (due to crystalization) . . .” to “The permeabilities of fractures are much higher or lower (due to crystalization) than that of surrounding matrix, . . .”. Please see it in the 4th line in the first paragraph of introduction.
- We replace “in the interface by “on the interface” in our whole paper.
- We change “the Darcy’s law” to “Darcy’s law”. Please see it in the 8th line of Page 2.
- We revised “and the existence and uniqueness of the mixed finite element approximation was analyzed” as “and the existence and uniqueness of the mixed finite element approximation were analyzed”. Please see it in the 12th line of Page 2.
- We change “error estimates for the two-grid method is discussed” as “error estimates for the two-grid method are discussed”. Please see it in the third line of Page 3.
- We change “Darcy law” to “Darcy’s law” above Equation (2.1) in Page 3.
- “the constant $\xi \in (1/2, 1]$ ” is replaced by “ ξ is a parameter with $\xi \in (1/2, 1]$ ”. Please see it in the 6th line of Page 4.
- “ $a(\cdot, \cdot)$ is coercive and continuity” is replaced by “ $a(\cdot, \cdot)$ is coercive and continuous”. Please see it above Equation (4.3) in Page 7.
- In Tables 1-8, in order to avoid confusion, errors of pressure and velocity “ e^p ” and “ e^u ” are replaced by “ $p - p^h$ ” and “ $\mathbf{u} - \mathbf{u}^h$ ” in the coupled method, and by “ $p - \hat{p}^h$ ” and “ $\mathbf{u} - \hat{\mathbf{u}}^h$ ” in the two-grid decoupled method. Please see them in Pages 13-15.
- We revised “errors and convergence rates is shown in the following tables” as “errors and convergence rates are shown in the following tables”. Please see it in Page 15.

2. Comment: More specifically, the novelty of the work is not properly established in the context of existing literature in this area.

Response: Thank you for your comments and suggestions.

In the third paragraph of section 2, we add the advantage of the proposed two-grid decoupled algorithm. “Traditional finite element methods for fracture models result in coupled and even nonlinear discrete problems. Computational cost and numerical difficulty increase largely as the mesh size decreases. There are many advantages for

us to use the decoupled algorithm for mixed models. Firstly, we just need solve the coupled problem on a coarse grid, and on the fine grid, we solve local problems in subdomains individually, so numerical difficulty is reduced in comparison with the coupled method. Secondly, optimized local solvers can be applied to local problems. Especially for the Darcy-Forchheimer/Darcy fracture model, since the equation of the fracture is nonlinear, traditional methods will result in a coupled nonlinear discrete problems. But if the decoupled method is used, we only solve nonlinear system in the fracture instead of in the whole domain. Finally, local problems on the fine grid can be solved in a parallel multiprocess, and computational cost will be further reduced.” Please see it in Page 2.

In Remark 4.1 of section 4, we summarize the theoretical analysis of the coupled and decoupled algorithms for the mixed Darcy/Darcy fracture model. If we choose a proper coarse grid such that $h = H^{3/2}$, the decoupled two-grid algorithm holds an optimal convergence rate for the pressure p on the H^1 semi-norm, so we theoretically prove that the proposed decoupled algorithm retains the same order of approximation accuracy as the coupled method.

In section 6, we implement the coupled and the two-grid decoupled algorithms for the mixed Darcy/Darcy fracture model and the mixed Darcy-Forchheimer/Darcy fracture model. By comparing numerical results of two algorithms, the two-grid decoupled algorithm maintains the same order of accuracy as the coupled method, and computation times of decoupled method are greatly reduced, especially for the mixed nonlinear Darcy-Forchheimer/Darcy fracture model, which shows the efficiency of the proposed decoupled algorithm.

3. Comment: The mathematical description of their two-grid algorithm for the fracture model presented in section 3 and error estimate in section 4 is little adhoc.

Response: Thank you for your comments and suggestions.

In section 3, we firstly give the triangulation of the computational domain and the corresponding finite element spaces are introduced. Then the coupled method and the two-grid decoupled method are established in Algorithm 1 and Algorithm 2, respectively.

In section 4, the main goal of this section is described in the first paragraph. In Theorem 4.1, the theoretical result for the coupled method is proved, and based on this theorem, we obtain the theoretical analysis for the proposed two-grid decoupled algorithm. Finally, we give a remark of this section to summarize the main theoretical results for the proposed algorithm.

4. Comment: Based on remark 4.1 on Page 9, the optimal convergence of their two-grid algorithm requires a correlation between coarse and fine grid sizes, which doesn’t necessarily make it a decoupled algorithm.

Response: Thank you for your comments and suggestions. In the proposed two-grid decoupled algorithm, we use a coarse grid approximation to the interface coupling conditions, so error estimates of the pressure and velocity are related to the size of the coarse grid, as in articles [4,17]. In order to obtain the optimal convergence rates for the pressure and velocity, we should choose a proper coarse grid such that $h = H^{3/2}$. With the properly chosen coarse grid, the mixed Darcy/Darcy or Darcy-Forchheimer/Darcy fracture problem in the fine grid is decoupled to local problems defined on the fracture and in the surrounding domains, as shown on Page 6 and Page 12. Hence, the most efficient and optimized local solvers can be individually developed for local problems, and even they can be implemented on a process of parallelism, which is suitable for today’s computing environment.

For traditional coupled methods of the mixed Darcy/Darcy or Darcy-Forchheimer/Darcy fracture model, numerical difficulty and computation cost increase as the mesh size decreases. For the proposed two-grid decoupled algorithm, theoretical analysis shows that it maintains the same order of approximation accuracy as the coupled algorithm, and numerical experiments show that computation times of decoupled method are greatly reduced compared to the coupled method, even though a coupled solver on a coarse grid is required, especially for the mixed nonlinear Darcy-Forchheimer/Darcy fracture model. When we apply the proposed decoupled algorithm to this fracture model, the local problem only on the fracture is nonlinear, so the Picard iteration is required just on the fracture instead of the whole computational domain.

Finally, we would like to thank the anonymous reviewers for their valuable comments that improved the quality

of our paper. We hope that the revised manuscript has addressed all the concerns and is worth publishing.

A Two-Grid Decoupled Algorithm for Fracture Models

Shuangshuang Chen¹, Hongxing Rui^{1,*}

¹ *School of Mathematics, Shandong University,
Jinan, Shandong, 250100, China.*

Abstract. In this paper, we consider a two-grid decoupled algorithm for two categories of fracture models. In the mixed Darcy/Darcy fracture model, fluid flow in fractures as well as in the surrounding medium is governed by Darcy's law. And in the mixed Darcy-Forchheimer/Darcy fracture model, flow in fractures is governed by Darcy-Forchheimer's law while that in surrounding matrix is governed by Darcy's law. In the proposed two-grid method, we use a coarse grid approximation to the interface coupling conditions for decoupling mixed problems in fractures and surrounding matrix. Error estimates show that the two-grid decoupled algorithm retains the same order of approximation accuracy as the coupled algorithm for the pressure p on H^1 semi-norm and the velocity \mathbf{u} on $(L^2)^2$ norm. Numerical experiments are carried out to verify the accuracy and efficiency of the decoupled algorithm, in which the computation times are reduced greatly compared to the coupled method.

Key words: Fracture models; two-grid method; decoupling; Darcy's law; Darcy-Forchheimer's law

Mathematics Subject Classification(2010): 65N12; 65N15; 65N30

1 Introduction

In this paper, we consider a single phase fluid flow in porous media with fractures, which has aroused increasing interest of researchers [1, 2, 6, 15, 16]. Modeling flow in porous media is difficult and the corresponding mathematical problem is complicated. In particular, fractures are taken into account. The permeabilities of fractures are much higher or lower (due to crystalization) than that of surrounding matrix, thus fractures play important roles on flow in the media acting as privileged channels or barriers. In addition, there are interactions between fractures and surrounding domains. Compared to the size of the whole domain, the fracture generally has at least one dimension with a very small width, and an idea treating fractures as $(n - 1)$ -dimensional interfaces in the n -dimensional domain was proposed in [1] for high permeability fracture models. In [15], a model was presented to generalize the earlier models and it was improved to handle both large and small permeability of fractures. For models with more permeable fractures, fluid tends to flow into fractures and along them. Fractures can be seen as fast pathways in this case. The normal component of the velocity should not be expected to be continuous across fractures. While for models with less permeable fractures, it is easy to see that the fluid has a tendency to avoid fractures.

The work of second author is supported by the National Natural Science Foundation of China Grant (No. 91330106 , 11671233)

*Corresponding author: hxrui@sdu.edu.cn.

Fractures act as geological barriers. The pressure will not be identical on both sides of fractures. Hence, nonstandard Robin type conditions on the interface were proposed in the fracture model of [15], which coupled a flow equation along the fracture with equations in surrounding domains. We also refer to [2, 6, 12, 16] for similar models. For all of the above models, the linear Darcy's law is used as the constitutive law for flow in fractures as well as in the surrounding domains. However, for high-ranged velocity, Darcy's law cannot fit well with experiments, and a nonlinear correction term should be added, the Forchheimer term [5, 21]. For fractures with large enough permeability, Darcy's law will be replaced by Darcy-Forchheimer's law. A model coupling Darcy-Forchheimer flow in the fracture and Darcy flow in the rest of the domain was carried out in [7], but the pressure was assumed to be continuous in this model. In [11](2014), a similar model without the continuity of pressure was derived, and the existence and uniqueness of the mixed finite element approximation were analyzed. There are also some researches on numerical methods of fracture models, such as an extended finite element method in [8], the mixed finite element with domain decomposition method in [10], the mixed finite element method with nonconforming grid in [6], and a block-centered finite difference method in [13]. In our paper, a decoupled two-grid algorithm is proposed to decouple the aforementioned fracture models in [15] and [11], using the coarse grid approximations on the interface. The decoupled local problems can be solved individually, and even on parallel processors, which is efficient and convenient.

The fracture model is one of multi-modeling problems consisting of different equations in fractures and surrounding domains, which are coupled via interface conditions. The aforementioned numerical approaches solve coupled fracture models directly. However, different equations defined in different regions are varied in type, such as coupling linear and nonlinear systems, and interface conditions include variables in different domains, which results in very complex algebraic structures. Another approach is to decouple mixed models firstly, and then local problems are solved by local solvers. There are some decoupling methods based on domain decomposition, for example, Quarteroni and Valli [19], Lagrange multiplier techniques [9], which have been widely used for multi-modeling problems. In [23] and [24], Xu proposed a new two-grid discretization technique for solving nonsymmetric and indefinite partial differential equations. Then in [17] and [4], the two-grid method was successfully applied to decouple multimodel problems, the mixed Stokes/Darcy model and the mixed Navier-Stokes/Darcy model. As shown in [17], the basic idea of the two-grid algorithm is to first solve a coupled problem on a much coarser grid, and then we get rough approximations of variables defined on the interface, which can be used to decouple the mixed model on the fine grid. So this procedure is consist of a coupled solver on the coarse grid and a decoupled local solver on the fine grid. More details about the two-grid method can be seen in [14, 20, 22].

In this paper, we will apply the two-grid decoupled algorithm to the mixed Darcy/Darcy model in [15] and the mixed Darcy-Forchheimer/Darcy model in [11]. Traditional finite element methods for fracture models result in coupled and even nonlinear discrete problems. Computational cost and numerical difficulty increase largely as the mesh size decreases. There are many advantages for us to use the decoupled algorithm for mixed models. Firstly, we just need solve the coupled problem on a coarse grid, and on the fine grid, we solve local problems in subdomains individually, so numerical difficulty is reduced in comparison with the coupled method. Secondly, optimized local solvers can be applied to local problems. Especially for the Darcy-Forchheimer/Darcy fracture model, since the equation of the fracture is nonlinear, traditional methods will result in a coupled nonlinear discrete problems. But if the decoupled method is used, we only solve nonlinear system in the fracture instead of in the whole domain. Finally, local problems on the fine grid can be solved in a parallel multiprocess, and computational cost will be further reduced.

The rest of this paper is organized as follows. In section 2, the fracture model coupling Darcy flow in both the fracture and surrounding matrix is described. And some notations are introduced.

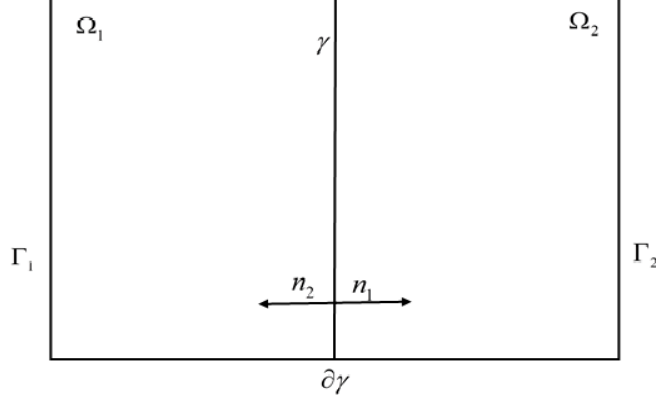


Figure 1: The domain of the fracture model

In section 3, the two-grid decoupled algorithm using a coarse grid approximation on the interface is proposed for the Darcy/Darcy fracture model. In section 4, error estimates for the proposed two-grid decoupled method are discussed, which shows that the two-grid decoupled method maintains the same order of convergence for pressure and velocity as the coupled method. In section 5, we extend the two-grid decoupled algorithm to the mixed Darcy-Forchheimer/Darcy fracture model. In section 6, numerical experiments for both coupled fracture models are carried out. Numerical results confirm our theoretical analysis, and computational time of decoupled method is reduced greatly compared to the coupled one. Finally, we give a brief conclusion of our work in section 7.

2 The mixed Darcy/Darcy fracture model

We firstly consider the mixed Darcy/Darcy fracture model derived in [15], which couples 2-dimensional linear elliptic equations in surrounding domains with a 1-dimensional linear elliptic equation on the fracture. For simplicity, let $\Omega = [a_1, a_2] \times [b_1, b_2]$ be a rectangular domain in \mathbb{R}^2 with the boundary Γ and let $\gamma = \{x = x_f\} \times [b_1, b_2] \subset \Omega$ be a one-dimensional surface as shown in Figure 1. Ω is separated by γ into two bounded sub-domains:

$$\Omega_1 = [a_1, x_f] \times [b_1, b_2], \text{ and } \Omega_2 = (x_f, a_2] \times [b_1, b_2],$$

$$\Omega \subset \mathbb{R}^2, \Omega \setminus \gamma = \Omega_1 \cup \Omega_2, \Gamma = \partial\Omega.$$

Denote by Γ_i the part of the boundary of Ω_i in common with the boundary of Ω , i.e., $\Gamma_i = \partial\Omega_i \cap \Gamma$, $i = 1, 2$. We define the velocity and pressure on $\Omega_i, i = 1, 2$ and γ by \mathbf{u}_i, p_i and u_f, p_f , respectively. We consider the following fracture problem, in which the flow in both the fracture and the surrounding matrix is governed by Darcy's law together with the conservation property.

$$\begin{aligned} \mathbf{u}_i &= -\mathbf{K}_i \nabla p_i & \text{in } \Omega_i, & \quad i = 1, 2, \\ \operatorname{div} \mathbf{u}_i &= q_i & \text{in } \Omega_i, & \quad i = 1, 2, \\ u_f &= -k_{f,y} d \frac{\partial p_f}{\partial y} & \text{in } \gamma, & \\ \frac{\partial u_f}{\partial y} &= q_f + (\mathbf{u}_1 \cdot \mathbf{n}_1|_\gamma + \mathbf{u}_2 \cdot \mathbf{n}_2|_\gamma) & \text{in } \gamma, & \quad (2.1) \\ -\xi \mathbf{u}_i \cdot \mathbf{n}_i + \alpha_f p_i &= \alpha_f p_f - (1 - \xi) \mathbf{u}_{i+1} \cdot \mathbf{n}_{i+1} & \text{in } \gamma, & \\ p_i &= \bar{p}_i & \text{on } \Gamma_i, & \quad i = 1, 2, \\ p_f &= \bar{p}_f & \text{on } \partial\gamma, & \end{aligned}$$

where \mathbf{n}_i is the unit normal vector on the interface γ directed outward from Ω_i , $\mathbf{n}_1 = -\mathbf{n}_2$. In this paper, we assume that $\mathbf{K}_i, i = 1, 2, \mathbf{K}_f = \text{diag}(k_{f,x}, k_{f,y})$ are symmetric matrices representing the permeability of flow in $\Omega_i, i = 1, 2$ and γ , and there exist constants $k_{\max} > k_{\min} > 0$ such that

$$k_{\min}|\zeta|^2 \leq \zeta^T \mathbf{K}_i \zeta \leq k_{\max}|\zeta|^2, \quad \forall \zeta \in \mathbb{R}^2,$$

$$k_{\min} \leq (k_{f,y}d), (k_{f,x}/d) \leq k_{\max}.$$

The parameter d denotes the thickness of the fracture, the coefficient $\alpha_f = 2k_{f,x}/d$, and ξ is a parameter with $\xi \in (1/2, 1]$. The index i varies in $\mathbb{Z}/2\mathbb{Z}$ satisfying $2 + 1 = 1$.

The fifth equation in (2.1) represents the Robin boundary conditions on the interface γ , which can be rewritten as follows,

$$\begin{aligned} \mathbf{u}_2 \cdot \mathbf{n}_2|_\gamma + \mathbf{u}_1 \cdot \mathbf{n}_1|_\gamma &= \frac{\alpha_f}{2\xi - 1}(p_2|_\gamma + p_1|_\gamma - 2p_f), \\ \mathbf{u}_2 \cdot \mathbf{n}_2|_\gamma - \mathbf{u}_1 \cdot \mathbf{n}_1|_\gamma &= \alpha_f(p_2|_\gamma - p_1|_\gamma). \end{aligned} \quad (2.2)$$

Furthermore, by summing and subtracting two equations in (2.2), we can obtain,

$$\mathbf{u}_i \cdot \mathbf{n}_i|_\gamma = \frac{\alpha_f}{2\xi - 1}(\xi p_i|_\gamma + (1 - \xi)p_{i+1}|_\gamma - p_f), \quad i = 1, 2. \quad (2.3)$$

For simplicity, we will consider the homogenous boundary conditions on p in the following analysis, i.e., $\bar{p}_i = 0$ and $\bar{p}_f = 0$, and the non-homogenous case can be handled by a lifting function. For any non-negative integer m and number $s \geq 1$, denote by $W^{m,s}$ the classical Sobolev space, equipped with the standard semi-norm $|\cdot|_{W^{m,s}}$ and norm $\|\cdot\|_{W^{m,s}}$. When $s = 2$, this is the Hilbert space H^m . We introduce the following spaces.

$$\begin{aligned} W_i &= \{w_i \in H^1(\Omega_i) \mid w_i = 0, \text{ on } \Gamma_i\}, \quad i = 1, 2, \\ W_f &= \{w_f \in H^1(\gamma) \mid w_f = 0, \text{ on } \partial\gamma\}, \\ W &= \{w = (w_1, w_2, w_f) \in W_1 \times W_2 \times W_f\}, \end{aligned} \quad (2.4)$$

with the following semi-norm and norm

$$|p|_W = \sum_{i=1,2} |p_i|_{H^1(\Omega_i)} + |p_f|_{H^1(\gamma)},$$

and

$$\|p\|_W = \sum_{i=1,2} \|p_i\|_{H^1(\Omega_i)} + \|p_f\|_{H^1(\gamma)}.$$

The weak formulation of the fracture model (2.1) can be written as follows: Find $p = (p_1, p_2, p_f) \in W$ such that

$$a(p, w) = \sum_{i=1,2} (q_i, w_i)_{\Omega_i} + (q_f, w_f)_\gamma, \quad \forall w = (w_1, w_2, w_f) \in W, \quad (2.5)$$

where $a(\cdot, \cdot)$ is the bilinear form from $W \times W$ to R

$$\begin{aligned} a(p, w) &= \sum_{i=1,2} (\mathbf{K}_i \nabla p_i, \nabla w_i)_{\Omega_i} + \left(k_{f,y} d \frac{\partial p_f}{\partial y}, \frac{\partial w_f}{\partial y} \right)_\gamma \\ &\quad + \sum_{i=1,2} \left(\frac{\alpha_f}{2\xi - 1} (\xi p_i + (1 - \xi)p_{i+1} - p_f), w_i \right)_\gamma - \left(\frac{\alpha_f}{2\xi - 1} (p_1 + p_2 - 2p_f), w_f \right)_\gamma. \end{aligned} \quad (2.6)$$

It is easy to check the continuity of the bilinear form $a(\cdot, \cdot)$ over $W \times W$, and then we will verify that $a(\cdot, \cdot)$ is W-elliptic. For any $w = (w_1, w_2, w_f) \in W$,

$$\begin{aligned} a(w, w) &= \sum_{i=1,2} (\mathbf{K}_i \nabla w_i, \nabla w_i)_{\Omega_i} + \left(k_{f,y} d \frac{\partial w_f}{\partial y}, \frac{\partial w_f}{\partial y} \right)_{\gamma} \\ &\quad + \sum_{i=1,2} \left(\frac{\alpha_f}{2\xi - 1} (\xi w_i + (1 - \xi) w_{i+1} - w_f), w_i - w_f \right)_{\gamma}. \end{aligned}$$

For the last term in the above equation, under the assumption of the permeability \mathbf{K}_f , we have $\alpha_f = \frac{2k_{f,x}}{d} \geq 2k_{\min}$,

$$\begin{aligned} &\sum_{i=1,2} \left(\frac{\alpha_f}{2\xi - 1} (\xi w_i + (1 - \xi) w_{i+1} - w_f), w_i - w_f \right)_{\gamma} \\ &= \sum_{i=1,2} \left(\frac{\alpha_f}{2\xi - 1} (\xi(w_i - w_f) + (1 - \xi)(w_{i+1} - w_f)), w_i - w_f \right)_{\gamma} \\ &= \xi \sum_{i=1,2} \left(\frac{\alpha_f}{2\xi - 1} (w_i - w_f), w_i - w_f \right)_{\gamma} + 2(1 - \xi) \left(\frac{\alpha_f}{2\xi - 1} (w_1 - w_f), w_2 - w_f \right)_{\gamma} \\ &\geq \frac{2k_{\min}}{(2\xi - 1)} (2\xi - 1) \sum_{i=1,2} (w_i - w_f, w_i - w_f)_{\gamma} \\ &= 2k_{\min} \sum_{i=1,2} \|w_i - w_f\|_{L^2(\gamma)}^2. \end{aligned}$$

And by the assumption of \mathbf{K}_i and $k_{f,y}d$, we get

$$a(w, w) \geq k_{\min} \left(\sum_{i=1,2} |w_i|_{H^1(\Omega_i)}^2 + |w_f|_{H^1(\gamma)}^2 \right) + 2k_{\min} \sum_{i=1,2} \|w_i - w_f\|_{L^2(\gamma)}^2.$$

And by the Poincare inequality,

$$\sum_{i=1,2} \|w_i\|_{L^2(\Omega_i)} + \|w_f\|_{L^2(\gamma)} \leq C \left(\sum_{i=1,2} |w_i|_{H^1(\Omega_i)} + |w_f|_{H^1(\gamma)} \right).$$

There exists a constant C satisfying

$$a(w, w) \geq C \left(\sum_{i=1,2} \|w_i\|_{H^1(\Omega_i)}^2 + \|w_f\|_{H^1(\gamma)}^2 + \sum_{i=1,2} \|w_i - w_f\|_{L^2(\gamma)}^2 \right).$$

Hence, the model problem (2.5)-(2.6) has a unique solution.

3 The two-grid algorithm for the fracture model

Suppose that \mathcal{T}_i^h is a triangulation of the subdomain $\Omega_i, i = 1, 2$, with the longest diameter of elements h_i . And \mathcal{T}_1^h and \mathcal{T}_2^h align on the fracture γ to form a partition of γ ,

$$\mathcal{T}_f^h : \textcolor{blue}{b}_1 = y_0 < y_1 < \cdots < y_n = \textcolor{blue}{b}_2.$$

Define

$$y_{\ell+1/2} = \frac{y_\ell + y_{\ell+1}}{2}, \quad \text{and} \quad \sigma_{\ell+1/2} = (y_\ell, y_{\ell+1}), \quad \ell = 0, \dots, n-1.$$

Let $\mathcal{T}^h = \cup_{i=1,2} \mathcal{T}_i^h \cup \mathcal{T}_f^h$ with $h = \max_{i=1,2} h_i$ be the partition of the whole computational domain. For the coupled fracture model (2.1), we consider the conforming linear finite element space $W^h = W_1^h \times W_2^h \times W_f^h$ defined on \mathcal{T}^h . For $i = 1, 2$, $W_i^h \subset W_i$,

$$W_i^h = \left\{ w_i^h \in H^1(\Omega_i) : w_i^h \text{ is linear for any } K \in \mathcal{T}_h^i, w_i^h = 0, \text{ on } \Gamma_i \right\}.$$

And $W_f^h \subset W_f$,

$$W_f^h = \left\{ w_f^h \in H^1(\gamma) : w_f^h \text{ is linear in } \sigma_{\ell+1/2}, \ell = 0, \dots, n-1, w_f^h = 0, \text{ on } \partial\gamma \right\}.$$

The coupled finite element discretization for the mixed Darcy/Darcy fracture model reads as follows.

Algorithm 1. Find $p^h = (p_1^h, p_2^h, p_f^h) \in W^h$ such that

$$a(p^h, w^h) = \sum_{i=1,2} (q_i, w_i^h)_{\Omega_i} + (q_f, w_f^h)_\gamma, \quad \forall w^h = (w_1^h, w_2^h, w_f^h) \in W^h. \quad (3.1)$$

We then propose a two-grid algorithm for decoupling the mixed Darcy/Darcy fracture model using a coarse grid approximation on the interface.

Algorithm 2.

1. Solve a coarse grid coupled problem: Find $p^H = (p_1^H, p_2^H, p_f^H) \in W^H$ such that

$$a(p^H, w^H) = \sum_{i=1,2} (q_i, w_i^H)_{\Omega_i} + (q_f, w_f^H)_\gamma, \quad \forall w^H = (w_1^H, w_2^H, w_f^H) \in W^H. \quad (3.2)$$

2. Solve a decoupled fine grid problem: Find $\hat{p}^h = (\hat{p}_1^h, \hat{p}_2^h, \hat{p}_f^h) \in W^h$ satisfying for any $w^h = (w_1^h, w_2^h, w_f^h) \in W^h$,

$$\begin{aligned} & \sum_{i=1,2} (\mathbf{K}_i \nabla \hat{p}_i^h, \nabla w_i^h)_{\Omega_i} + \left(k_{f,y} d \frac{\partial \hat{p}_f^h}{\partial y}, \frac{\partial w_f^h}{\partial y} \right)_\gamma + \sum_{i=1,2} \frac{\xi}{2\xi-1} (\alpha_f \hat{p}_i^h, w_i^h)_\gamma + \frac{2}{2\xi-1} (\alpha_f \hat{p}_f^h, w_f^h)_\gamma \\ &= - \sum_{i=1,2} \frac{1-\xi}{2\xi-1} (\alpha_f p_{i+1}^H, w_i^h)_\gamma + \sum_{i=1,2} \frac{1}{2\xi-1} (\alpha_f p_f^H, w_i^h)_\gamma + \sum_{i=1,2} \frac{1}{2\xi-1} (\alpha_f p_i^H, w_f^h)_\gamma \\ &+ \sum_{i=1,2} (q_i, w_i^h)_{\Omega_i} + (q_f, w_f^h)_\gamma. \end{aligned} \quad (3.3)$$

We can easily check that the decoupled fine grid problem is well-posed and it is equivalent to three local problems defined on three sub-domains Ω_1, Ω_2 and γ .

The discrete Darcy problem defined in the matrix $\Omega_i, i = 1, 2$:

$$(\mathbf{K}_i \nabla \hat{p}_i^h, \nabla w_i^h)_{\Omega_i} + \frac{\xi}{2\xi-1} (\alpha_f \hat{p}_i^h, w_i^h)_\gamma = - \frac{1-\xi}{2\xi-1} (\alpha_f p_{i+1}^H, w_i^h)_\gamma + \frac{1}{2\xi-1} (\alpha_f p_f^H, w_i^h)_\gamma + (q_i, w_i^h)_{\Omega_i}. \quad (3.4)$$

The discrete Darcy problem defined on the fracture γ :

$$\left(k_{f,y} d \frac{\partial \hat{p}_f^h}{\partial y}, \frac{\partial w_f^h}{\partial y} \right)_\gamma + \frac{2}{2\xi-1} (\alpha_f \hat{p}_f^h, w_f^h)_\gamma = \sum_{i=1,2} \frac{1}{2\xi-1} (\alpha_f p_i^H, w_f^h)_\gamma + (q_f, w_f^h)_\gamma. \quad (3.5)$$

4 Error estimate

The main purpose of this section is to analyze error estimations of the coupled and the two-grid decoupled algorithms for the mixed Darcy/Darcy fracture model. We will prove that the two-grid decoupled method retains the same order of accuracy with the coupled method, with a properly chosen coarse grid. In our analysis, the letter C will be used to denote a positive constant with independence of mesh size and indicate difference values at its difference appearances.

Theorem 4.1 *For the coupled method Algorithm 1, we suppose that $p_i \in H^2(\Omega_i), i = 1, 2$, and $p_f \in H^2(\gamma)$ are exact solutions to the mixed Darcy/Darcy fracture model (2.1), then the following error estimates hold.*

$$\begin{aligned} \sum_{i=1,2} |p_i - p_i^h|_{H^1(\Omega_i)} + |p_f - p_f^h|_{H^1(\gamma)} &\leq Ch, \\ \sum_{i=1,2} \|p_i - p_i^h\|_{L^2(\Omega_i)} + \|p_f - p_f^h\|_{L^2(\gamma)} &\leq Ch^2. \end{aligned} \quad (4.1)$$

Proof. Subtracting the discrete problem (3.1) from (2.5), we have the following error equation.

$$a(p - p^h, w^h) = 0, \quad \forall w^h \in W^h. \quad (4.2)$$

Let $p^I = (p_1^I, p_2^I, p_f^I) \in W^h$ be the orthogonal L^2 projection such that

$$\begin{aligned} \int_{\Omega_i} (p_i^I - p_i) w_i d\mathbf{x} &= 0, \quad \forall w_i \in W_i^h, \quad i = 1, 2, \\ \int_{\gamma} (p_f^I - p_f) w_f ds &= 0, \quad \forall w_f \in W_f^h, \end{aligned}$$

with the following properties

$$\begin{aligned} h|p_i^I - p_i|_{W^{1,s}(\Omega_i)} + \|p_i^I - p_i\|_{L^s(\Omega_i)} &\leq Ch^2 \|p_i\|_{W^{2,s}(\Omega_i)}, \quad i = 1, 2, \\ h|p_f^I - p_f|_{W^{1,s}(\gamma)} + \|p_f^I - p_f\|_{L^s(\gamma)} &\leq Ch^2 \|p_f\|_{W^{2,s}(\gamma)}. \end{aligned}$$

In (4.2), taking $w^h = p^h - p^I \in W^h$, we obtain

$$a(p^I - p^h, p^I - p^h) = -a(p - p^I, p^I - p^h).$$

Since $a(\cdot, \cdot)$ is coercive and continuous over W ,

$$\begin{aligned} &\left(\sum_{i=1,2} |p_i^I - p_i^h|_{H^1(\Omega_i)}^2 + |p_f^I - p_f^h|_{H^1(\gamma)}^2 + \sum_{i=1,2} \|(p_i^I - p_i^h) - (p_f^I - p_f^h)\|_{L^2(\gamma)}^2 \right)^{1/2} \\ &\leq C \left(\sum_{i=1,2} |p_i^I - p_i|_{H^1(\Omega_i)} + |p_f^I - p_f|_{H^1(\gamma)} + \sum_{i=1,2} \|(p_i^I - p_i) - (p_f^I - p_f)\|_{L^2(\gamma)} \right). \end{aligned} \quad (4.3)$$

For the last term in the right side of (4.3), by the trace inequality, we have

$$\begin{aligned} \|p_i^I - p_i\|_{L^2(\gamma)}^2 &= \sum_{\ell=0}^n \|p_i^I - p_i\|_{L^2(\sigma_{\ell+1/2})}^2 \leq C \left(\sum_{K \in \mathcal{T}_i^h} h^{-1} \|p_i^I - p_i\|_{L^2(K)}^2 + \sum_{K \in \mathcal{T}_i^h} h |p_i^I - p_i|_{H^1(K)}^2 \right) \\ &\leq Ch^3 \|p_i\|_{H^2(\Omega_i)}^2. \end{aligned}$$

Together with the properties of the projection p^I , the error estimate for pressure p on the H^1 semi-norm holds.

$$\begin{aligned} & \sum_{i=1,2} |p_i - p_i^h|_{H^1(\Omega_i)} + |p_f - p_f^h|_{H^1(\gamma)} + \sum_{i=1,2} \|(p_i - p_i^h) - (p_f - p_f^h)\|_{L^2(\gamma)} \\ & \leq Ch \left(\sum_{i=1,2} \|p_i\|_{H^2(\Omega_i)} + \|p_f\|_{H^2(\gamma)} \right). \end{aligned}$$

We then turn our attention to the analysis of the pressure p on the L^2 norm. Using the Aubin-Nitsche duality technique [3], we consider the following dual problem defined by the error $p - p^h$,

$$a(v, w) = \sum_{i=1,2} (p_i - p_i^h, w_i)_{\Omega_i} + (p_f - p_f^h, w_f)_{\gamma}, \quad \forall w = (w_1, w_2, w_f) \in W. \quad (4.4)$$

We assume that $v = (v_1, v_2, v_f) \in H^2(\Omega_1) \times H^2(\Omega_2) \times H^2(\gamma)$ is the solution to the dual problem, and

$$\sum_{i=1,2} \|v_i\|_{H^2(\Omega_i)} + \|v_f\|_{H^2(\gamma)} \leq C \left(\sum_{i=1,2} \|p_i - p_i^h\|_{L^2(\Omega_i)} + \|p_f - p_f^h\|_{L^2(\gamma)} \right). \quad (4.5)$$

Taking $w = p - p^h$ in (4.4),

$$a(v, p - p^h) = \sum_{i=1,2} (p_i - p_i^h, p_i - p_i^h)_{\Omega_i} + (p_f - p_f^h, p_f - p_f^h)_{\gamma}.$$

Comparing (2.5) and (3.1), we have

$$a(p - p^h, v^h) = 0, \quad \forall v^h \in W^h.$$

Hence, using the estimate of the pressure on the H^1 semi-norm,

$$\begin{aligned} & \sum_{i=1,2} \|p_i - p_i^h\|_{L^2(\Omega_i)}^2 + \|p_f - p_f^h\|_{L^2(\gamma)}^2 \\ & = a(p - p^h, v - v^h) \\ & \leq \left(\sum_{i=1,2} |p_i - p_i^h|_{H^1(\Omega_i)} + |p_f - p_f^h|_{H^1(\gamma)} + \sum_{i=1,2} \|(p_i - p_i^h) - (p_f - p_f^h)\|_{L^2(\gamma)} \right) \\ & \quad \left(\sum_{i=1,2} |v_i - v_i^h|_{H^1(\Omega_i)} + |v_f - v_f^h|_{H^1(\gamma)} + \sum_{i=1,2} \|(v_i - v_i^h) - (v_f - v_f^h)\|_{L^2(\gamma)} \right) \\ & \leq Ch^2 \left(\sum_{i=1,2} \|v_i\|_{H^2(\Omega_i)} + \|v_f\|_{H^2(\gamma)} \right) \\ & \leq Ch^2 \left(\sum_{i=1,2} \|p_i - p_i^h\|_{L^2(\Omega_i)} + \|p_f - p_f^h\|_{L^2(\gamma)} \right). \end{aligned} \quad (4.6)$$

The result holds. □

We can immediately obtain the following estimates by Theorem 4.1

$$\begin{aligned} \sum_{i=1,2} |p_i^h - p_i^H|_{H^1(\Omega_i)} + |p_f^h - p_f^H|_{H^1(\gamma)} &\leq CH, \\ \sum_{i=1,2} \|p_i^h - p_i^H\|_{L^2(\Omega_i)} + \|p_f^h - p_f^H\|_{L^2(\gamma)} &\leq CH^2. \end{aligned} \quad (4.7)$$

Theorem 4.2 *Let $p^h = (p_1^h, p_2^h, p_f^h)$ and $\hat{p}^h = (\hat{p}_1^h, \hat{p}_2^h, \hat{p}_f^h)$ be solutions to the coupled method Algorithm 1 and two-grid decoupled method Algorithm 2, respectively. The following error estimate holds.*

$$\sum_{i=1,2} |p_i^h - \hat{p}_i^h|_{H^1(\Omega_i)} + |p_f^h - \hat{p}_f^h|_{H^1(\gamma)} \leq CH^{3/2}.$$

Proof. Subtracting the discrete decoupled problem (3.3) from the discrete coupled one (3.1), yields

$$\begin{aligned} &\sum_{i=1,2} (\mathbf{K}_i \nabla(p_i^h - \hat{p}_i^h), \nabla w_i^h)_{\Omega_i} + \left(k_{f,y} d \frac{\partial(p_f^h - \hat{p}_f^h)}{\partial y}, \frac{\partial w_f^h}{\partial y} \right)_\gamma + \sum_{i=1,2} \frac{\xi}{2\xi - 1} \left(\alpha_f(p_i^h - \hat{p}_i^h), w_i^h \right)_\gamma \\ &+ \frac{2}{2\xi - 1} \left(\alpha_f(p_f^h - \hat{p}_f^h), w_f^h \right)_\gamma \\ = & - \sum_{i=1,2} \frac{1 - \xi}{2\xi - 1} \left(\alpha_f(p_{i+1}^h - p_{i+1}^H), w_i^h \right)_\gamma + \sum_{i=1,2} \frac{1}{2\xi - 1} \left(\alpha_f(p_f^h - p_f^H), w_i^h \right)_\gamma \\ &+ \sum_{i=1,2} \frac{1}{2\xi - 1} \left(\alpha_f(p_i^h - p_i^H), w_i^h \right)_\gamma. \end{aligned} \quad (4.8)$$

In the above equation, taking $w^h = (p_1^h - \hat{p}_1^h, p_2^h - \hat{p}_2^h, p_f^h - \hat{p}_f^h) \in W^h$, we get

$$\begin{aligned} &k_{\min} \left(\sum_{i=1,2} |p_i^h - \hat{p}_i^h|_{H^1(\Omega_i)}^2 + |p_f^h - \hat{p}_f^h|_{H^1(\gamma)}^2 \right) + \sum_{i=1,2} \frac{2k_{\min}\xi}{2\xi - 1} \|p_i^h - \hat{p}_i^h\|_{L^2(\gamma)}^2 + \frac{4k_{\min}}{2\xi - 1} \|p_f^h - \hat{p}_f^h\|_{L^2(\gamma)}^2 \\ \leq & \sum_{i=1,2} \frac{2k_{\max}(1 - \xi)}{2\xi - 1} \|p_{i+1}^h - p_{i+1}^H\|_{L^2(\gamma)} \|p_i^h - \hat{p}_i^h\|_{L^2(\gamma)} + \sum_{i=1,2} \frac{2k_{\max}}{2\xi - 1} \|p_f^h - p_f^H\|_{L^2(\gamma)} \|p_i^h - \hat{p}_i^h\|_{L^2(\gamma)} \\ &+ \sum_{i=1,2} \frac{2k_{\max}}{2\xi - 1} \|p_i^h - p_i^H\|_{L^2(\gamma)} \|p_f^h - \hat{p}_f^h\|_{L^2(\gamma)} \\ \leq & \frac{k_{\min}}{2} \left(\sum_{i=1,2} \|p_i^h - \hat{p}_i^h\|_{L^2(\gamma)}^2 + \|p_f^h - \hat{p}_f^h\|_{L^2(\gamma)}^2 \right) + C \left(\sum_{i=1,2} \|p_i^h - p_i^H\|_{L^2(\gamma)}^2 + \|p_f^h - p_f^H\|_{L^2(\gamma)}^2 \right). \end{aligned} \quad (4.9)$$

Using the trace inequality, we have $\|p_i^h - p_i^H\|_{L^2(\gamma)} \leq CH^{3/2}$. Together with $\|p_f^h - p_f^H\|_{L^2(\gamma)} \leq CH^2$, the following estimate holds.

$$\sum_{i=1,2} |p_i^h - \hat{p}_i^h|_{H^1(\Omega_i)} + |p_f^h - \hat{p}_f^h|_{H^1(\gamma)} + \sum_{i=1,2} \|p_i^h - \hat{p}_i^h\|_{L^2(\gamma)} + \|p_f^h - \hat{p}_f^h\|_{L^2(\gamma)} \leq CH^{3/2}. \quad (4.10)$$

□

Remark 4.1 *Together with Theorem 4.1, we can immediately get the error estimate between the exact solution p and the two-grid decoupled finite element approximation \hat{p}^h .*

$$\sum_{i=1,2} |p_i - \hat{p}_i^h|_{H^1(\Omega_i)} + |p_f - \hat{p}_f^h|_{H^1(\gamma)} \leq Ch + CH^{3/2}.$$

If we choose a proper coarse grid such that $h = H^{3/2}$, the above inequality shows that the numerical approximation of the decoupled two-grid algorithm holds an optimal convergence rate $O(h)$ for the pressure p on the H^1 semi-norm. And compared to Theorem 4.1, we know that the proposed two-grid decoupled algorithm retains the same order of approximation accuracy as the coupled method in our theoretical analysis. Therefore, using a coarse grid approximation to the interface, we efficiently decouple the mixed Darcy/Darcy fracture model to local problems defined in subdomains, which can be independently solved by applying optimized local solvers.

5 The mixed Darcy-Forchheimer/Darcy fracture model

In this section, we consider the mixed Darcy-Forchheimer/Darcy fracture model derived in [7,11], in which flow is governed by Darcy-Forchheimer's law in the fracture and by Darcy's law in surrounding matrix. When the permeability in the fracture is much higher than that in the surrounding domains, the flow rate in the fracture is very high. And in this case, experiments show that a nonlinear correction need be added in the fracture. So the fracture model combining Darcy flow in surrounding matrix and Darcy-Forchheimer flow in the fracture fits well, which is described as follows in detail.

$$\begin{aligned}
\alpha_i \mathbf{u}_i + \nabla p_i &= 0 & \text{in } \Omega_i, & \quad i = 1, 2, \\
\operatorname{div} \mathbf{u}_i &= q_i & \text{in } \Omega_i, & \quad i = 1, 2, \\
p_i &= \bar{p}_i & \text{on } \Gamma_i, & \quad i = 1, 2, \\
(\alpha_\gamma + \beta_\gamma |u_f|) u_f + \frac{\partial p_f}{\partial y} &= g & \text{in } \gamma, & \\
\frac{\partial u_f}{\partial y} &= q_f + (\mathbf{u}_1 \cdot \mathbf{n}_1|_\gamma + \mathbf{u}_2 \cdot \mathbf{n}_2|_\gamma) & \text{in } \gamma, & \\
p_f &= \bar{p}_f & \text{on } \partial\gamma, &
\end{aligned} \tag{5.1}$$

and the interface conditions

$$p_i = p_f + \kappa (\mathbf{u}_i \cdot \mathbf{n}_i - (1 - \xi) \mathbf{u}_{i+1} \cdot \mathbf{n}_{i+1}) \quad \text{in } \gamma, \quad i = 1, 2, \tag{5.2}$$

where α_i , $i = 1, 2$, and α_γ are related to the inverse of the permeability on the sub-domains Ω_i , $i = 1, 2$, and the fracture γ , respectively, β_γ is the Forchheimer coefficient, and κ defined in γ is the coefficient scalar function related to the fracture width and inversely to the normal component of the permeability on the fracture. In this paper, we suppose that α_i is symmetric matrix and positive defined

$$\begin{aligned}
\underline{\alpha}_i |\zeta|^2 &\leq \zeta^T \alpha_i \zeta \leq \bar{\alpha}_i |\zeta|^2, \quad \forall \zeta \in \mathbb{R}^2, \\
\underline{\alpha}_\gamma &\leq \alpha_\gamma \leq \bar{\alpha}_\gamma, \\
\underline{\beta}_\gamma &\leq \beta_\gamma \leq \bar{\beta}_\gamma, \\
\underline{\kappa} &\leq \kappa \leq \bar{\kappa}.
\end{aligned}$$

Similar to [18], for the Darcy-Forchheimer equation on the fracture of (5.1), we get $|u_f|$ in the following form,

$$|u_f| = \frac{-\alpha_\gamma + \sqrt{\alpha_\gamma^2 + 4\beta_\gamma \left| \frac{\partial p_f}{\partial y} - g \right|}}{2\beta_\gamma}.$$

Then the flux u_f can be written as follows

$$u_f = -\frac{2}{\alpha_\gamma + \sqrt{\alpha_\gamma^2 + 4\beta_\gamma \left| \frac{\partial p_f}{\partial y} - g \right|}} \left(\frac{\partial p_f}{\partial y} - g \right).$$

And for the Robin boundary condition on the interface,

$$\mathbf{u}_2 \cdot \mathbf{n}_2|_\gamma + \mathbf{u}_1 \cdot \mathbf{n}_1|_\gamma = \frac{1}{(2\xi - 1)\kappa} (p_2|_\gamma + p_1|_\gamma - 2p_f).$$

Hence, the system of flow on the fracture is described as follows.

$$-\frac{\partial}{\partial y} \left(\frac{2 \left(\frac{\partial p_f}{\partial y} - g \right)}{\alpha_\gamma + \sqrt{\alpha_\gamma^2 + 4\beta_\gamma \left| \frac{\partial p_f}{\partial y} - g \right|}} \right) = q_f + \frac{1}{(2\xi - 1)\kappa} (p_2|_\gamma + p_1|_\gamma - 2p_f), \quad \text{in } \gamma. \quad (5.3)$$

For simplicity, we assume that $g = 0$ in our analysis. And denote by W the finite element method as follows.

$$\begin{aligned} W_i &= \{w_i \in H^1(\Omega_i) \mid w_i = 0, \text{ on } \Gamma_i\}, \quad i = 1, 2, \\ W_f &= \{w_f \in W^{1,3/2}(\gamma) \cap L^2(\gamma) \mid w_f = 0, \text{ on } \partial\gamma\}, \\ W &= \{w = (w_1, w_2, w_f) \in W_1 \times W_2 \times W_f\}, \end{aligned} \quad (5.4)$$

with the following semi-norm and norm

$$\begin{aligned} |p|_W &= \sum_{i=1,2} |p_i|_{H^1(\Omega_i)} + |p_f|_{W^{1,3/2}(\gamma)}, \\ \|p\|_W &= \sum_{i=1,2} \|p_i\|_{H^1(\Omega_i)} + \|p_f\|_{W^{1,3/2}(\gamma)}. \end{aligned}$$

The weak formulation of the fracture model (5.1) reads: Find $p = (p_1, p_2, p_f) \in W$ such that

$$a(p, w) = \sum_{i=1,2} (q_i, w_i)_{\Omega_i} + (q_f, w_f)_\gamma, \quad \forall w = (w_1, w_2, w_f) \in W, \quad (5.5)$$

where $a(\cdot, \cdot) : W \times W \mapsto \mathbb{R}$

$$\begin{aligned} a(p, w) &= \sum_{i=1,2} (\alpha_i^{-1} \nabla p_i, \nabla w_i)_{\Omega_i} + \left(\frac{2}{\alpha_\gamma + \sqrt{\alpha_\gamma^2 + 4\beta_\gamma \left| \frac{\partial p_f}{\partial y} \right|}} \frac{\partial p_f}{\partial y}, \frac{\partial w_f}{\partial y} \right)_\gamma \\ &\quad + \sum_{i=1,2} \left(\frac{1}{(2\xi - 1)\kappa} (\xi p_i + (1 - \xi)p_{i+1} - p_f), w_i \right)_\gamma - \left(\frac{1}{(2\xi - 1)\kappa} (p_1 + p_2 - 2p_f), w_f \right)_\gamma. \end{aligned} \quad (5.6)$$

The only difference between the forms $a(\cdot, \cdot)$ in (2.6) and (5.6) is the second term. And for the nonlinear system (5.6), it is easy to check that there exist constants c and C satisfying

$$c \left| \frac{\partial p_f}{\partial y} \right|_{L^{3/2}(\gamma)}^{3/2} \leq \left(\frac{2}{\alpha_\gamma + \sqrt{\alpha_\gamma^2 + 4\beta_\gamma \left| \frac{\partial p_f}{\partial y} \right|}} \frac{\partial p_f}{\partial y}, \frac{\partial p_f}{\partial y} \right)_\gamma \leq C \left| \frac{\partial p_f}{\partial y} \right|_{L^{3/2}(\gamma)}^{3/2}. \quad (5.7)$$

The coupled finite element discretization for the fracture model with the nonlinear Darcy-Forchheimer equation on the fracture is proposed.

Algorithm 3. Find $p^h = (p_1^h, p_2^h, p_f^h) \in W^h$ such that

$$a(p^h, w^h) = \sum_{i=1,2} (q_i, w_i^h)_{\Omega_i} + (q_f, w_f^h)_\gamma, \quad \forall w^h = (w_1^h, w_2^h, w_f^h) \in W^h. \quad (5.8)$$

And we also study the two-grid algorithm for decoupling this nonlinear problem using a coarse grid approximation on the interface.

Algorithm 4.

1. Solve a coarse grid coupled problem: Find $p^H = (p_1^H, p_2^H, p_f^H) \in W^H$ such that

$$a(p^H, w^H) = \sum_{i=1,2} (q_i, w_i^H)_{\Omega_i} + (q_f, w_f^H)_{\gamma}, \quad \forall w^H = (w_1^H, w_2^H, w_f^H) \in W^H. \quad (5.9)$$

2. Solve a decoupled fine grid problem: Find $\hat{p}^h = (\hat{p}_1^h, \hat{p}_2^h, \hat{p}_f^h) \in W^h$ satisfying for any $w^h = (w_1^h, w_2^h, w_f^h) \in W^h$,

$$\begin{aligned} & \sum_{i=1,2} (\alpha_i^{-1} \nabla \hat{p}_i^h, \nabla w_i^h)_{\Omega_i} + \left(\frac{2}{\alpha_{\gamma} + \sqrt{\alpha_{\gamma}^2 + 4\beta_{\gamma} |\frac{\partial \hat{p}_f^h}{\partial y}|}} \frac{\partial \hat{p}_f^h}{\partial y}, \frac{\partial w_f^h}{\partial y} \right)_{\gamma} \\ & + \sum_{i=1,2} \left(\frac{\xi}{(2\xi - 1)\kappa} \hat{p}_i^h, w_i^h \right)_{\gamma} + \left(\frac{2}{(2\xi - 1)\kappa} \hat{p}_f^h, w_f^h \right)_{\gamma} \\ = & - \sum_{i=1,2} \left(\frac{(1 - \xi)}{(2\xi - 1)\kappa} p_{i+1}^H, w_i^h \right)_{\gamma} + \sum_{i=1,2} \left(\frac{1}{(2\xi - 1)\kappa} p_f^H, w_i^h \right)_{\gamma} \\ & + \sum_{i=1,2} \left(\frac{1}{(2\xi - 1)\kappa} p_i^H, w_f^h \right)_{\gamma} + \sum_{i=1,2} (q_i, w_i^h)_{\Omega_i} + (q_f, w_f^h)_{\gamma}. \end{aligned} \quad (5.10)$$

Similar to the decoupled method for the linear system (3.4)-(3.5), we can rewrite (5.10) into the following three local problems.

The discrete linear Darcy problem defined in the matrix $\Omega_i, i = 1, 2$:

$$(\alpha_i^{-1} \nabla \hat{p}_i^h, \nabla w_i^h)_{\Omega_i} + \left(\frac{\xi}{(2\xi - 1)\kappa} \hat{p}_i^h, w_i^h \right)_{\gamma} = - \left(\frac{(1 - \xi)}{(2\xi - 1)\kappa} p_{i+1}^H, w_i^h \right)_{\gamma} + \left(\frac{1}{(2\xi - 1)\kappa} p_f^H, w_i^h \right)_{\gamma} + (q_i, w_i^h)_{\Omega_i}. \quad (5.11)$$

The discrete nonlinear Darcy-Forchheimer problem defined on the fracture γ :

$$\left(\frac{2}{\alpha_{\gamma} + \sqrt{\alpha_{\gamma}^2 + 4\beta_{\gamma} |\frac{\partial \hat{p}_f^h}{\partial y}|}} \frac{\partial \hat{p}_f^h}{\partial y}, \frac{\partial w_f^h}{\partial y} \right)_{\gamma} + \left(\frac{2}{(2\xi - 1)\kappa} \hat{p}_f^h, w_f^h \right)_{\gamma} = \sum_{i=1,2} \left(\frac{1}{(2\xi - 1)\kappa} p_i^H, w_f^h \right)_{\gamma} + (q_f, w_f^h)_{\gamma}. \quad (5.12)$$

From the local problems (5.11)-(5.12), we can see that linear problems are solved in two subdomains Ω_1 and Ω_2 , and only the local problem defined in fracture γ is nonlinear, so iteration is required just on the fracture for the Darcy-Forchheimer problem. Hence, the decoupled two-grid algorithm is especially convenient and time-saving for the nonlinear system.

6 Numerical Experiment

In this section, numerical examples are carried out to verify the accuracy and efficiency of the proposed two-grid approach for the mixed Darcy/Darcy fracture model and the mixed Darcy-Forchheimer/Darcy model. For simplicity, the computational domain for examples is rectangle, i.e., $\Omega = [-1, 1] \times [0, 1]$, and $\gamma = \{x = 0\} \times [0, 1]$ is the fracture. The triangulation of Ω is formed by bisecting rectangles of the same shapes. In order to show the convergence rates of the two-grid method, exact solutions (\mathbf{u}, p) to numerical examples are known, which also can be used to determine the right-hand side functions and Dirichlet boundary conditions of fracture models. The

finite element spaces are constructed by the linear and constant elements for the pressure p and the velocity \mathbf{u} , respectively. The convergence rates of pressure p on the H^1 semi-norm and velocity \mathbf{u} on the $(L^2)^2$ norm are all expected to be of first-order accuracy for both the coupled method and the two-grid decoupled method with $h = H^{3/2}$.

6.1 Numerical examples for Problem (2.1)

We firstly test three numerical examples with higher, lower or even anisotropic fracture permeability for the mixed Darcy/Darcy fracture model. The permeability and exact solutions are show as follows. Errors and convergence rates of pressure and velocity are compared for the coupled and decoupled algorithms in Tables 1-6. In addition, Gauss-Seidel iteration is used to solve the algebraic systems of coupled and decoupled finite element methods, and computational times are also compared to show the efficiency of the decoupled two-grid algorithm.

Example 1. The tensors of permeability on the fracture and the surrounding domains are all isotropic and constant, $\mathbf{K}_1 = \mathbf{K}_2 = \mathbf{I}$, $\mathbf{K}_f = 20\mathbf{I}$, where \mathbf{I} is the two dimensional identity matrix. The width of the fracture $d = 10^{-3}$ and $\xi = 4/5$. The fracture permeability is sufficiently large, so the fracture acts as a fast pathway and the flow tends to flow rapidly on the fracture. The exact solution of Example 1 is given as follows, and error estimates and convergence rates for Algorithms 1 and 2 are shown in Tables 1 and 2, respectively.

$$\begin{cases} p_1 = (x + 1) \sin(2\pi y) \\ p_2 = -(4x - (1 - 3/(4 * 10^4))) \sin(2\pi y) \\ p_f = \sin(2\pi y). \end{cases}$$

Table 1

Error estimates and convergence rates for Algorithm 1

| h | $ p - p^h _W$ | Rate | $\ \mathbf{u} - \mathbf{u}^h\ _{(L^2(\Omega))^2}$ | Rate | Time |
|----------|---------------|--------|---|--------|-------------|
| 2^{-2} | 0.369767 | - | 0.367025 | - | 0.0020s |
| 2^{-3} | 0.168760 | 1.1316 | 0.183759 | 0.9994 | 0.0086s |
| 2^{-4} | 0.081184 | 1.0557 | 0.091916 | 0.9998 | 0.0539s |
| 2^{-5} | 0.040128 | 1.0166 | 0.045963 | 0.9999 | 0.2472s |
| 2^{-6} | 0.020004 | 1.0043 | 0.022982 | 1.0000 | 3.1001s |
| 2^{-7} | 0.009995 | 1.0011 | 0.011491 | 1.0000 | 53.9027s |
| 2^{-8} | 0.004996 | 1.0002 | 0.005745 | 1.0000 | 1120.0023s |
| 2^{-9} | 0.002498 | 1.0001 | 0.002872 | 1.0000 | 19317.8788s |

Table 2

Error estimates and convergence rates for Algorithm 2

| $h = H^{3/2}$ | H | $ p - \hat{p}^h _W$ | Rate | $\ \mathbf{u} - \hat{\mathbf{u}}^h\ _{(L^2(\Omega))^2}$ | Rate | Time |
|---------------|----------|---------------------|--------|---|--------|-------------|
| 2^{-3} | 2^{-2} | 0.196694 | - | 0.196704 | - | 0.0082s |
| 2^{-6} | 2^{-4} | 0.024248 | 3.0200 | 0.024251 | 3.0200 | 2.9547s |
| 2^{-9} | 2^{-6} | 0.002988 | 3.0206 | 0.002993 | 3.0183 | 11076.0313s |

Example 2. $\mathbf{K}_1 = \mathbf{K}_2 = 10\mathbf{I}$, and $\mathbf{K}_f = 10^{-3}\mathbf{I}$, $d = 0.001$ and $\xi = 4/5$. In this case, the fracture permeability is much smaller than the surrounding matrix permeability, so the fluid barely flows through the fracture and the fracture can be seen as geologic barrier. Results of coupled and decoupled algorithms are presented in Table 3 and Table 4, respectively.

$$\begin{cases} p_1 = (x + 1) \sin(2\pi y) \\ p_2 = -(3x + 9) \sin(2\pi y) \\ p_f = 2 \sin(2\pi y). \end{cases}$$

Table 3

Error estimates and convergence rates for Algorithm 1

| h | $ p - p^h _W$ | Rate | $\ \mathbf{u} - \mathbf{u}^h\ _{(L^2(\Omega))^2}$ | Rate | Time |
|----------|---------------|--------|---|--------|-------------|
| 2^{-2} | 0.349013 | - | 0.282293 | - | 0.3052s |
| 2^{-3} | 0.140336 | 1.3143 | 0.134201 | 1.0727 | 0.4499s |
| 2^{-4} | 0.066227 | 1.0834 | 0.066245 | 1.0185 | 0.9464s |
| 2^{-5} | 0.032590 | 1.0229 | 0.033018 | 1.0045 | 2.8728s |
| 2^{-6} | 0.016227 | 1.0060 | 0.016496 | 1.0011 | 11.8176s |
| 2^{-7} | 0.008105 | 1.0015 | 0.008246 | 1.0003 | 79.12588s |
| 2^{-8} | 0.004051 | 1.0003 | 0.004123 | 1.0001 | 1070.7029s |
| 2^{-9} | 0.002025 | 1.0001 | 0.002061 | 1.0000 | 15456.3896s |

Table 4

Error estimates and convergence rates for Algorithm 2

| $h = H^{3/2}$ | H | $ p - \hat{p}^h _W$ | Rate | $\ \mathbf{u} - \hat{\mathbf{u}}^h\ _{(L^2(\Omega))^2}$ | Rate | Time |
|---------------|----------|---------------------|--------|---|--------|------------|
| 2^{-3} | 2^{-2} | 0.141561 | - | 0.134517 | - | 0.0106s |
| 2^{-6} | 2^{-4} | 0.016260 | 3.1220 | 0.016501 | 3.0271 | 1.6215s |
| 2^{-9} | 2^{-6} | 0.002026 | 3.0046 | 0.002061 | 3.0008 | 8360.2546s |

Example 3. We test an example with anisotropic fracture permeability,

$$\mathbf{K}_1 = \mathbf{K}_2 = 10\mathbf{I}, \quad \text{and} \quad \mathbf{K}_f = \begin{pmatrix} 10 & 0 \\ 0 & 10^{-3} \end{pmatrix}.$$

The width of the fracture $d = 10^{-3}$, and $\xi = 2/3$.

$$\begin{cases} p_1 = (x + 1) \sin(2\pi y) \\ p_2 = -(2x + 4) \sin(2\pi y) \\ p_f = \sin(2\pi y). \end{cases}$$

Table 5

Error estimates and convergence rates for Algorithm 1

| h | $ p - p^h _W$ | Rate | $\ \mathbf{u} - \mathbf{u}^h\ _{(L^2(\Omega))^2}$ | Rate | Time |
|----------|---------------|--------|---|--------|-------------|
| 2^{-2} | 0.320980 | - | 0.283537 | - | 0.0020s |
| 2^{-3} | 0.137929 | 1.2186 | 0.135265 | 1.0677 | 0.0075s |
| 2^{-4} | 0.066287 | 1.0571 | 0.066827 | 1.0173 | 0.0261s |
| 2^{-5} | 0.032781 | 1.0158 | 0.033315 | 1.0042 | 0.2222s |
| 2^{-6} | 0.016343 | 1.0041 | 0.016645 | 1.0010 | 3.1018s |
| 2^{-7} | 0.008166 | 1.0010 | 0.008321 | 1.0002 | 54.1243s |
| 2^{-8} | 0.004082 | 1.0002 | 0.004160 | 1.0001 | 1138.9655s |
| 2^{-9} | 0.002041 | 1.0001 | 0.002080 | 1.0000 | 17615.2500s |

Table 6

Error estimates and convergence rates for Algorithm 2

| $h = H^{3/2}$ | H | $ p - \hat{p}^h _W$ | Rate | $\ \mathbf{u} - \hat{\mathbf{u}}^h\ _{(L^2(\Omega))^2}$ | Rate | Time |
|---------------|----------|---------------------|--------|---|--------|-------------|
| 2^{-3} | 2^{-2} | 0.139436 | - | 0.135683 | - | 0.0083s |
| 2^{-6} | 2^{-4} | 0.016382 | 3.0894 | 0.016655 | 3.0262 | 2.7181s |
| 2^{-9} | 2^{-6} | 0.002041 | 3.0042 | 0.002089 | 2.9946 | 10125.3466s |

From Tables 2, 4 and 6, we know that convergence rates of pressure p on the H^1 semi-norm and the velocity \mathbf{u} on the $(L^2)^2$ norm maintain first-order reduction for the decoupled algorithm, which is consistent with our theoretical analysis. Meanwhile, by comparing the first table and the second table of every example, the two-grid decoupled algorithm holds the same order accuracy as the coupled method for pressure and velocity, and we note that computation times of decoupled method are almost reduced by half compared to the coupled method, even though a coupled solver on a coarse grid is required.

6.2 Numerical examples for Problem (5.1)

Next, numerical experiments of the mixed Darcy-Forchheimer/Darcy fracture model are carried out. Both coupled and two-grid decoupled methods result in nonlinear algebraic systems for this model, so Picard iterations with zero initial guesses are used. For Algorithm 3, the iteration is required in the whole computational domain and the stopping criterion is $\|P^{m+1} - P^m\|_{L^2(\Omega)} \leq 10^{-8}$, where P^m is the nodal-value vector of the pressure for the m th iterate, while for the two-grid decoupled method Algorithm 4, the Picard iteration is just used for pressure only on the fracture γ and the stopping criterion is $\|P_f^{m+1} - P_f^m\|_{L^2(\gamma)} \leq 10^{-8}$.

Example 4. We take $\alpha_i = \mathbf{I}$, $\alpha_\gamma = \beta_\gamma = 1$, $\kappa = 1$ and $\xi = \frac{4}{5}$, for simplicity. The exact solution is described as follows and errors and convergence rates are shown in the following tables.

$$\begin{cases} p_1 = (x + 1) \sin(2\pi y), \\ p_2 = -(4x + 2) \sin(2\pi y), \\ p_f = \sin(2\pi y). \end{cases}$$

$$\mathbf{u}_1 = - \begin{pmatrix} \sin(2\pi y) \\ 2\pi(x+1)\cos(2\pi y) \end{pmatrix}, \quad u_f = -2\pi \cos(2\pi y), \quad \text{and} \quad \mathbf{u}_2 = - \begin{pmatrix} 4\sin(2\pi y) \\ 2\pi(4x+2)\cos(2\pi y) \end{pmatrix}.$$

And the right-hand side functions

$$\begin{cases} q_1 = 4\pi^2(x+1)\sin(2\pi y), & \text{in } \Omega_1, \\ q_2 = -4\pi^2(4x+2)\sin(2\pi y), & \text{in } \Omega_2 \\ q_f = (4\pi^2+5)\sin(2\pi y), & \text{in } \gamma, \\ g = -4\pi^2|\cos(2\pi y)|\cos(2\pi y), & \text{in } \gamma. \end{cases}$$

Table 7

Error estimates and convergence rates for Algorithm 3

| h | $ p - p^h _W$ | Rate | $\ \mathbf{u} - \mathbf{u}^h\ _{(L^2(\Omega))^2}$ | Rate | Time |
|----------|---------------|--------|---|--------|-----------|
| 2^{-2} | 0.414460 | - | 0.287813 | - | 0.0540s |
| 2^{-3} | 0.159646 | 1.3764 | 0.139340 | 1.0465 | 0.0778s |
| 2^{-4} | 0.071645 | 1.1559 | 0.069033 | 1.0132 | 0.0847s |
| 2^{-5} | 0.034764 | 1.0432 | 0.034435 | 1.0034 | 0.2743s |
| 2^{-6} | 0.017248 | 1.0112 | 0.017207 | 1.0009 | 1.0933s |
| 2^{-7} | 0.008607 | 1.0028 | 0.008602 | 1.0002 | 5.3310s |
| 2^{-8} | 0.004301 | 1.0007 | 0.004301 | 1.0001 | 29.7199s |
| 2^{-9} | 0.002150 | 1.0001 | 0.002150 | 1.0000 | 173.9807s |

Table 8

Error estimates and convergence rates for Algorithm 4

| $h = H^{3/2}$ | H | $ p - \hat{p}^h _W$ | Rate | $\ \mathbf{u} - \hat{\mathbf{u}}^h\ _{(L^2(\Omega))^2}$ | Rate | Time |
|---------------|----------|---------------------|--------|---|--------|---------|
| 2^{-3} | 2^{-2} | 0.165276 | - | 0.140696 | - | 0.0703s |
| 2^{-6} | 2^{-4} | 0.017647 | 3.2274 | 0.017366 | 3.0182 | 0.1645s |
| 2^{-9} | 2^{-6} | 0.002161 | 3.0298 | 0.002156 | 3.0101 | 7.2832s |

For the mixed Darcy-Forchheimer/Darcy fracture model, compared numerical results in the above two tables, the two-grid decoupled algorithm holds the same order of approximation accuracy as the coupled method for the pressure p on the H^1 semi-norm and the velocity \mathbf{u} on the $(L^2)^2$ norm. In the proposed two-grid decoupled method, since the local problem only on the fracture is nonlinear, the Picard iteration is required just on the fracture instead of the whole computational domain. The computation time of the decoupled method is greatly reduced. Hence, for the mixed nonlinear Darcy-Forchheimer/Darcy fracture model, the two-grid decoupled algorithm is numerically more efficient, and it enables easy implementation.

7 Conclusion

We have proposed a two-grid decoupled algorithm for the mixed Darcy/Darcy fracture model and the mixed Darcy-Frochheimer/Darcy fracture model, in which a coupled system on a coarse grid is firstly solved, and then the mixed problem in a fine grid is decoupled using approximations of variables defined on the interface. Optimized local solvers and even a parallel process can be applied to local problems. Error estimates show that the proposed decoupled method holds the same order of approximation accuracy as the coupled method for the pressure and velocity. Numerical experiments are carried out for both fracture models, and numerical results confirm our theoretical analysis. In addition, compared to the coupled method, the computational time of the decoupled method is greatly reduced, especially for the nonlinear Darcy-Frochheimer/Darcy fracture model, since we only need do iterations on the fracture instead of the whole domain. Hence, both theoretical analysis and numerical experiments show the efficiency and effectiveness of the two-grid decoupled method for fracture models.

References

- [1] C. Alboin, J. Jaffre, J. Roberts, and C. Serres. Domain decomposition for flow in fractured porous media. *Domain Decomposition Methods in Sciences and Engineering*, pages 365–373, 1999.
- [2] P. Angot, F. Boyer, and F. Hubert. Asymptotic and numerical modelling of flows in fractured porous media. *Mathematical Modelling and Numerical Analysis*, 43(2):239–275, 2009.
- [3] F. Brezzi and M. Fortin. Mixed and hybrid finite element methods. *Springer-Verlag*, 1991.
- [4] M. Cai, M. Mu, and J. Xu. Numerical solution to a mixed Navier-Stokes/Darcy model by the two-grid approach. *SIAM Journal on Numerical Analysis*, 47(5):3325–3338, 2009.
- [5] P. Forchheimer. Wasserbewegung durch boden. *Zeitschrift des Vereines deutscher Ingenieure*, 45(5):1781–1788, 1901.
- [6] N. Frih, V. Martin, J. Roberts, and A. Saada. Modeling fractures as interfaces with nonmatching grids. *Computational Geosciences*, pages 1–18, 2012.
- [7] N. Frih, J. Roberts, and A. Saada. Modeling fractures as interfaces: a model for Forchheimer fractures. *Computational Geosciences*, 12(1):91–104, 2008.
- [8] A. Fumagalli and A. Scotti. Numerical modelling of multiphase subsurface flow in the presence of fractures. *Communications in Applied and Industrial Mathematics*, 3(1), 2011.
- [9] R. Glowinski, T. Pan, and T. Hesla. A distributed Lagrangian multiplier/fictitious domain method for particulate flow. *International Journal of Multiphase Flow*, 25:775–794, 1999.
- [10] T. Hoang, C. Japhet, M. Kern, and J. Roberts. Space-time domain decomposition for reduced fracture models in mixed formulation. *SIAM Journal on Numerical Analysis*, 54(1):288–316, 2016.
- [11] P. Knabner and J. Roberts. Mathematical analysis of a discrete fracture model coupling Darcy flow in the matrix with Darcy-Forchheimer flow in the fracture. *ESAIM: Mathematical Modelling and Numerical Analysis*, 48(5):1451–1472, 2014.

- [12] M. Lesinigo, C. D'Angelo, and A. Quarteroni. A multiscale Darcy-Brinkman model for fluid flow in fractured porous media. *Numerische Mathematik*, 117(4):717–752, 2011.
- [13] W. Liu and Z. Sun. A block-centered finite difference method for reduced fracture model in karst aquifer system. *Computers and Mathematics with Applications*, 74(6):1455–1470, 2017.
- [14] M. Marion and J. Xu. Error estimates on a new nonlinear galerkin method based on two-grid finite elements. *SIAM Journal on Numerical Analysis*, 32(4):1170–1184, 1995.
- [15] V. Martin, J. Jaffre, and J. Roberts. Modeling fractures and barriers as interfaces for flow in porous media. *SIAM Journal on Scientific Computing*, 26(5):1667–1691, 2005.
- [16] F. Morales and R. Showalter. The narrow fracture approximation by channeled flow. *Journal of Mathematical Analysis and Applications*, 365(1):320–331, 2010.
- [17] M. Mu and J. Xu. A two-grid method of a mixed Stokes-Darcy model for coupling fluid flow with porous media flow. *SIAM Journal on numerical analysis*, 45(5):1801–1813, 2007.
- [18] H. Pan and H. Rui. Mixed element method for two-dimensional Darcy-Forchheimer model. *Journal of Scientific Computing*, 52(3):563–587, 2012.
- [19] A. Quarteroni and A. Valli. Domain decomposition methods for partial differential equations. *Oxford University Press*, 1999.
- [20] H. Rui and W. Liu. A two-grid block-centered finite difference method for Darcy-Forchheimer flow in porous media. *SIAM Journal on Numerical Analysis*, 53(4):1941–1962, 2015.
- [21] H. Rui and H. Pan. A block-centered finite difference method for the Darcy-Forchheimer model. *SIAM Journal on Numerical Analysis*, 50(5):2612–2631, 2012.
- [22] J. Xu. Iterative methods by space decomposition and subspace correction. *Society for Industrial and Applied Mathematics*, 34(4):581–613, 1992.
- [23] J. Xu. A novel two-grid method for semilinear elliptic equations. *SIAM Journal on Scientific Computing*, 15(1):231–237, 1994.
- [24] J. Xu. Two-grid discretization techniques for linear and nonlinear PDEs. *SIAM Journal on Numerical Analysis*, 33(5):1759–1777, 1996.